$(e,3e)$ processes on two-electron atoms: Cusp conditions and scaling law

L. U. Ancarani,[1] C. Dal Cappello,[1] I. Charpentier,[2] K. V. Rodriguez,[3] and G. Gasaneo[3]
[1]*Laboratoire de Physique Moléculaire et des Collisions, Université Paul Verlaine - Metz, 57078 Metz, France*
[2]*Laboratoire de Physique et Mécanique des Matériaux, UMR CNRS 7554, Ile du Saulcy, 57045 Metz, France*
[3]*Departamento de Física, Universidad Nacional del Sur and Consejo Nacional de Investigaciones Científicas y Técnicas, 8000 Bahía Blanca, Buenos Aires, Argentina*
(Received 25 September 2008; published 11 December 2008)

We study the double ionization by electron impact of the ground state of heliumlike atoms and propose a scaling law for fully differential $(e,3e)$ cross sections. Within the first Born approximation, cross sections are calculated with a three-body Coulomb (3C) double-continuum wave function and initial states represented by highly accurate wave functions, which satisfy all two-body Kato cusp conditions. We first consider the helium atom in the kinematical and geometrical conditions of the only absolute, high incident energy, experimental data available: our calculations confirm unambiguously that satisfying or not Kato cusp conditions is not a relevant feature of the ground state. Other heliumlike atoms are then considered. Under similar conditions, cross sections for H^- are much larger than for helium while the reverse is true for positive ions; a comparison with the rare other theoretical calculations is performed. Finally, within our theoretical framework, we propose an approximate scaling law for $(e,3e)$ cross sections for heliumlike positive ions, and confirm it by calculations.

DOI: 10.1103/PhysRevA.78.062709 PACS number(s): 34.80.Dp, 32.80.Fb

I. INTRODUCTION

The theoretical study of the double ionization of atoms by electron impact [$(e,3e)$ experiments] allows one to gain information on correlated systems [1]. In the case of two-electron atomic targets, such as helium, one deals with a pure four-body Coulomb problem which, for high incident energies, can be reduced to a three-body problem from a theoretical point of view. However, even in this case, no exact wave function is known for either the scattering or the bound states. Hence, approximate wave functions are used, and $(e,3e)$ cross sections on helium obtained with a different theoretical description of the initial and final states are generally not in agreement with each other. Moreover, when these are compared with high energy absolute experimental data on helium [2,3], a rather confusing picture emerges; this is the subject of many recent studies (see, e.g., [4], and below). Many ingredients enter the calculation of fivefold differential cross sections (FDCS) and it is important to understand which one is important for the theoretical description of experimental data.

In this work, we take as final state the so-called three-body Coulomb (3C) [or Brauner-Briggs-Klar (BBK)] model [5,6] of the double continuum. This model has known limitations; however, it has the merit of diagonalizing the three-body Hamiltonian, and hence satisfies exactly the so-called Kato two-body cusp conditions [7], and has the correct asymptotic behavior when all interparticle distances are large. Moreover, being analytical, it is practical for studying the ionization of a variety of atoms and molecules. In the case of two-electron atoms considered here, the analytical character will allow us to investigate a scaling law for their double ionization by electron impact.

The first aim of this paper is to focus on the initial bound state of helium, and, in particular, on the role of its behavior near the two-body coalescence points. The cusp conditions have a fundamental importance at high energy regimes in photo-double ionization [8], and it is interesting to investigate whether the same is true in $(e,3e)$ processes. The second aim is to provide cross section predictions for $(e,3e)$ processes on two-electron ions belonging to the heliumlike isoelectronic sequence. While charged targets are experimentally more difficult to deal with, it is interesting to study the nuclear charge (Z) dependence of the cross sections shapes and magnitudes. Indeed, the relative importance of the electron-electron correlation in the initial state, with respect to the electron-nucleus interaction, is largest for the ion H^- and decreases as Z increases. For H^-, FDCSs larger than for helium are expected while the reverse is true for heliumlike positive ions. Scaling laws for heliumlike ions have been investigated for $(e,2e)$ [9] and $(\gamma,2e)$ [10,11] but not for $(e,3e)$ processes. Here we provide an approximate scaling law for FDCS, which is based on the 3C model.

Let us start from the helium atom. A great amount of ground state wave functions have been presented in the literature, and many different types of constructions have been used to approximately include the correlation. In most of the advanced trial functions (e.g., [12,13]) used in ionization studies, the variational parameters are optimized in order to yield a very accurate ground state energy, without any attention to the behavior near the two-body coalescence points or to the large distance behavior. In general they do not satisfy Kato's cusp conditions. On the other hand, relatively simpler functions (e.g., [14]) fulfilling these conditions have been proposed and used, but give—in comparison—a less accurate energy. In a recent publication [15], the role of the behavior of the ground state wave functions near the two-body coalescence points was investigated in $(e,3e)$ calculations for helium within the 3C model. To this effect, the authors have built new variational bound wave functions, which yield very accurate ground state energies and at the same time satisfy almost exactly Kato cusp conditions. The func-

 ©2008 The American Physical Society

tions were built as the sum of a relatively large number of products of exponentials in the three Hylleraas coordinates; since the authors found it very difficult to fulfill the cusp conditions locally, they use a weaker condition, i.e., an averaged formulation. In order to eliminate any doubts and provide a definitive answer on this issue, we construct and use here trial wave functions, which satisfy these conditions exactly. A first step towards this aim was presented recently [4] with the systematic use of trial wave functions satisfying the cusp conditions and with different functional and asymptotic behaviors; however, similarly to the Le Sech trial wave function [14], the ground state energy was still quite far from the numerically exact value. In this paper we shall consider two sets of trial functions, which yield accurate energies, in order to answer the question of whether or not the exact fulfillment of Kato's cusp conditions is important for describing the double ionization of helium at high incident energy.

For $(e,3e)$ processes on helium, calculated FDCSs can be compared with those measured by Lahmam-Bennani *et al.* [2,3] for high incident energy (5599 eV) and ejected energies of $E_1=E_2=10$ eV (small momentum transfer). These coplanar measurements allow one to make a detailed study—both in shape and magnitude—of the double ionization process. On the theoretical side, there have been published calculations based on the convergent close-coupling (CCC) approach [3,16], the *J*-matrix method to Faddeev-Merkuriev differential equations [17,18], a wave-packet evolution approach [19], and the distorted wave approaches (with the "pure" 3C model [15,20–24] or variants with effective charges [2,25,26]). Since the experimental energy of the incoming projectile is high, the comparison between the theoretical calculations and the measured data can be performed within the frame of a first Born approximation (FBA) in the interaction of the projectile with the target atom; indeed, explicit second Born calculations showed that little difference is observed with either the CCC [27] or a distorted wave approach [28]. Even within the FBA, the FDCSs obtained with a different theoretical description of the initial and final states are not in agreement with each other, and yield a rather confusing picture. The results presented within the Born-CCC approach, in combination with the 20-parameters Hylleraas function, show an overall shape agreement but present important magnitude disagreements (factor 3 [3] or 2.2 [16]). Calculations with the *J*-matrix approach [17] (where the initial and final wave functions are represented by an infinite expansion in a Laguerre basis) yield a reasonable agreement in the $(e,3e)$ cross sections magnitude, but to a lesser extent for their shapes. It should be noted that previous published calculations [18], where the pseudostates method was employed, showed important magnitude disagreements with experimental data, similarly to the CCC approach. Recently, a purely numerical calculation based on a wave-packet evolution approach has yielded results that are close, in both shape and magnitude, to those found with the CCC approach. Finally, the calculations performed with distorted wave approaches lead to different and divergent conclusions. The combination of the 3C model for the ejected electrons with different double bound initial wave functions yields results that depend on the level of correlation included in the initial state. Agreement in shape, but disagreement in magnitude (factor 1.5–2) is found when comparing the calculations and the experimental data [2], when highly correlated double bound wave functions like that of Le Sech [14], Bonham and Kohl [12], or Hylleraas-like are used for the initial channel [15,21,22,28]. On the other hand, overall agreement in both shape and magnitude is found [20,21,23] when using simpler wave functions, like that proposed by Pluvinage [29] (which diagonalizes the three two-body Coulomb potentials) or others with a similar analytical structure. It is worth underlying that all the 3C results, published by several groups and obtained with independent numerical codes, are consistent with each other (unfortunately some initial confusion arose from those published in [2] with a wrong magnitude).

The second aim of this paper is to investigate $(e,3e)$ cross sections for other two-electron ions. As far as we know, only few publications have dealt with the fully differential double ionization of heliumlike ions [30–35]; this is probably due to the lack of experimental data to compare with. Moreover, when the target is charged, the incident and scattered electrons should be described by Coulomb rather than plane waves, adding an extra difficulty to the theoretical model. If, however, the incident and scattered energies are sufficiently high, the corresponding Sommerfeld parameters are sufficiently small, so that the use of plane waves should not affect the results. For fixed kinematical and geometrical conditions, the cross sections for positive ions are expected to decrease as the nuclear charge increases. On the other hand, for H^-, cross sections larger than for helium are expected; calculations for this ion have been presented in [30–34]. In Ref. [30], the 3C model and an initial bound state of moderate quality were used. In the other publications [31–34], cross sections were calculated with simplified versions of the 3C model, in which the electron-electron interaction in the double continuum is either neglected (two Coulomb waves; named here 2C model) or described only by a Gamow factor (named here 2CG model). From the study of $(e,3e)$ cross sections, for example, for helium, it is known that such poor descriptions of the double continuum yield large differences when compared to the 3C model, and cannot reproduce the proper shapes and order of magnitude of experimental data. That said, the advantage of these simplified models of the double continuum permitted an interesting analytical investigation of the cross sections [31], or the inclusion of the projectile-target Coulomb interaction [32,33]. As Li^+ is concerned, FDCS have been calculated with a 2CG or 2C model [34,35]; in [35], the projectile-target Coulomb interaction is described with Coulomb waves. No other heliumlike positive ions have been studied, probably because the cross section is too small to be measurable. Hence, except for the work on H^- by Lamy *et al.* [30], only poor models of the double continuum have been considered for heliumlike ions. To fill this gap, we consider here the ions H^-, and Li^+ up to F^{7+}, and calculate FDCS within the 3C model and initial states of good quality. We shall first consider some of the kinematical and geometrical situations discussed in Refs. [30–35]. Next, we propose a situation in which the momentum transfer is kept constant. In this way, the cross sections for different targets will depend essentially on the target wave functions (and hence test the electron-electron correlation) and on the Sommerfeld parameters connected to the ejected electrons.

Finally, thanks to the analytical character of the 3C model and by adequately scaling the incident and the ejected energies, we identify an approximate scaling law for FDCS of heliumlike ions; our 3C calculations confirm its validity.

The rest of the paper is arranged as follows. In Sec. II, we briefly recall the theory for the evaluation of the fivefold differential cross section within the FBA. We next describe the final double continuum state in the 3C model, the double bound initial state wave functions considered, and the numerical technique used for the evaluation of cross sections. The results of our calculations for the helium atom and heliumlike ions are presented in Sec. III. A summary is given in Sec. IV.

Atomic units are used throughout ($\hbar=m_e=e=1$).

II. THEORY

The fully differential cross section for the ejection of two electrons from a two-electron atom by electron impact, the $(e,3e)$ reaction, is given by

$$\frac{d^5\sigma}{d\Omega_0 d\Omega_1 d\Omega_2 dE_1 dE_2} = (2\pi)^4 \frac{k_0 k_1 k_2}{k_i} |T_{fi}(\mathbf{k}_0,\mathbf{k}_1,\mathbf{k}_2)|^2. \quad (1)$$

Here $\mathbf{k}_i$ and $\mathbf{k}_0$ are the momenta of the incoming and outgoing projectile, $\mathbf{k}_1$ and $\mathbf{k}_2$ are the momenta of the ejected electrons after the collision (energy E_1, E_2); $d\Omega_0$, $d\Omega_1$, and $d\Omega_2$ denote, respectively, the solid angle elements for the scattered and the two ejected electrons. Let $\mathbf{r}_1$ and $\mathbf{r}_2$ represent the coordinates of two ejected electrons relative to the infinitely heavy nucleus, $\mathbf{r}_{12}=\mathbf{r}_1-\mathbf{r}_2$ the electron-electron relative vector, and $\mathbf{r_0}$ be the coordinate of the projectile. We shall restrict the present investigation to high incident energies E_i, so that the FBA for the transition matrix T_{fi} may be taken,

$$T_{fi} = \left\langle \frac{1}{(2\pi)^{3/2}} e^{i\mathbf{k}_0\cdot\mathbf{r}_0} \Psi_f^-(\mathbf{r}_1,\mathbf{r}_2) \middle| -\frac{Z}{r_0} + \frac{1}{|\mathbf{r}_0-\mathbf{r}_1|} + \frac{1}{|\mathbf{r}_0-\mathbf{r}_2|} \middle| \frac{1}{(2\pi)^{3/2}} e^{i\mathbf{k}_i\cdot\mathbf{r}_0} \Psi_i(\mathbf{r}_1,\mathbf{r}_2) \right\rangle, \quad (2)$$

where Z is the nuclear charge of the target. In this nine-dimensional integral, $\Psi_i(\mathbf{r}_1,\mathbf{r}_2)$ and $\Psi_f^-(\mathbf{r}_1,\mathbf{r}_2)$ are the exact initial and final channel wave functions for the two-electron system under consideration. The integration over the projectile coordinates ($\mathbf{r}_0$) can be performed analytically, using Bethe's integral, so that the transition amplitude reduces to a six-dimensional integral

$$T_{fi} = \frac{1}{2\pi^2 q^2} \langle \Psi_f^-(\mathbf{r}_1,\mathbf{r}_2) | -Z + e^{i\mathbf{q}\cdot\mathbf{r}_1} + e^{i\mathbf{q}\cdot\mathbf{r}_2} | \Psi_i(\mathbf{r}_1,\mathbf{r}_2) \rangle, \quad (3)$$

where $\mathbf{q}=\mathbf{k}_i-\mathbf{k}_0$ is the momentum transferred from the projectile to the target atom.

A. Final state

The dynamics of the two escaping electrons is represented here by the 3C model [6]. Taking into account exchange between electrons 1 and 2, this final state model is given by a symmetrized version of the C3 (or BBK) double-continuum wave function [5]

$$\Psi_f^- = N_{3C} \frac{1}{\sqrt{2}} [e^{i\mathbf{k}_1\cdot\mathbf{r}_1} e^{i\mathbf{k}_2\cdot\mathbf{r}_2} D(\alpha_1,\mathbf{k}_1,\mathbf{r}_1) D(\alpha_2,\mathbf{k}_2,\mathbf{r}_2) + e^{i\mathbf{k}_1\cdot\mathbf{r}_2} e^{i\mathbf{k}_2\cdot\mathbf{r}_1} D(\alpha_1,\mathbf{k}_1,\mathbf{r}_2) D(\alpha_2,\mathbf{k}_2,\mathbf{r}_1)] D(\alpha_{12},\mathbf{k}_{12},\mathbf{r}_{12}), \quad (4)$$

where

$$N_{3C} = e^{-(\pi/2)\alpha_1} \Gamma(1-i\alpha_1) e^{-(\pi/2)\alpha_2} \Gamma(1-i\alpha_2) \times e^{-(\pi/2)\alpha_{12}} \Gamma(1-i\alpha_{12}), \quad (5)$$

and the Coulomb distortion factor is given by

$$D(\alpha,\mathbf{k},\mathbf{r}) = {}_1F_1(i\alpha,1,-i(kr+\mathbf{k}\cdot\mathbf{r})), \quad (6)$$

The Sommerfeld parameters $\alpha_j=-Z/k_j$ $(j=1,2)$ and $\alpha_{12}=1/(2k_{12})$, with the relative momentum defined as $\mathbf{k}_{12}=(\mathbf{k}_1-\mathbf{k}_2)/2$, are directly related to the corresponding Coulomb potentials.

Since they are solutions of the same three-body Hamiltonian, the exact double-continuum state $\Psi_f^-(\mathbf{r}_1,\mathbf{r}_2)$ and the initial ground state $\Psi_i(\mathbf{r}_1,\mathbf{r}_2)$ are orthogonal. However, since in each case we do not know the exact solutions, orthogonality is broken, but can be restored through an artificial Schmidt orthogonalization

$$\langle \Psi_f^{-\perp}| = \langle \Psi_f^-| - \langle \Psi_f^-|\Psi_i\rangle \langle \Psi_i|. \quad (7)$$

In the case of helium, and for the $(e,3e)$ processes under scrutiny here, this operation does not much affect the shapes of the cross sections but gives a magnitude change of 10–15 % depending on the ejected angles [20,21]. On the other hand, the orthogonalization procedure has a dramatic effect for other two-electron ions; if the final state is not orthogonalized to the initial state an enormous spurious contribution appears in cross sections, giving rise to important shape and magnitude differences.

B. Initial state

The study of the Coulomb singularities has led Kato [7] to provide mathematical conditions that Ψ_i must satisfy (the so-called two-body cusp conditions) in order to eliminate these singularities.

$$\left[\frac{\partial\bar{\Psi}_i}{\partial r_1}\right]_{r_1\to 0} = -Z\Psi_i(0,r_2,r_{12}), \quad (8a)$$

$$\left[\frac{\partial\bar{\Psi}_i}{\partial r_2}\right]_{r_2\to 0} = -Z\Psi_i(r_1,0,r_{12}), \quad (8b)$$

$$\left[\frac{\partial\bar{\Psi}_i}{\partial r_{12}}\right]_{r_{12}\to 0} = \frac{1}{2}\Psi_i(r,r,0) \quad \text{with } r=\left|\frac{1}{2}(\mathbf{r}_1+\mathbf{r}_2)\right|, \quad (8c)$$

where $\bar{\Psi}_i$ means the average of Ψ_i over a very small sphere of radius r_1 (respectively, r_2 or r_{12}) keeping the other values

fixed. Relations (8a)–(8c) provide the linear behavior that Ψ_i must have close to the two-body coalescence points.

For the initial ground state Ψ_i we consider here two sets of trial wave functions, which depend on the three interparticle distances r_1, r_2, r_{12}. They are constructed with an *angularly correlated configuration interaction* approach, which uses two basis sets with functions satisfying exactly the three cusp conditions. The first one uses parameter-free basis functions, which diagonalize the three-body Hamiltonian [36]

$$\phi^{\mathrm{C3}}_{n_1,n_2,n_{12}} = \varphi_{n_1}(Z,r_1)\varphi_{n_2}(Z,r_2)\,{}_1F_1\left(-n_{12},2,-\frac{r_{12}}{n_{12}}\right),$$

where

$$\varphi_{n_i}(Z,r_j) = e^{-Zr_j/n_i}\,{}_1F_1\left(1-n_j,2,\frac{2Zr_j}{n_j}\right), \quad j=1,2, \tag{9}$$

are the unnormalized $L=0$ hydrogenic solutions of principal quantum numbers n_1 and n_2. The distortion factor ${}_1F_1[-n_{12},2,-\frac{r_{12}}{n_{12}}]$, with n_{12} a positive integer, emerges from the study of the double-bound analog of the C3 double-continuum function [37], and is actually a Laguerre polynomial $L^{(1)}_{n_{12}}(-\frac{r_{12}}{n_{12}})$; for the first two used below we have $L^{(1)}_1(-r_{12})=1+\frac{r_{12}}{2}$ and $L^{(1)}_2(-\frac{r_{12}}{2})=1+\frac{r_{12}}{2}+\frac{r_{12}^2}{24}$. The second basis functions, proposed by Gasaneo and Rodriguez and colleagues (GR) in [38,39], read

$$\phi^{\mathrm{GR}}_{n_1,n_2} = \varphi_{n_1}(Z,r_1)\varphi_{n_2}(Z,r_2)\frac{2\beta+1-e^{-\beta r_{12}}}{2\beta}.$$

They have a correlation factor tending to one at large electron-electron distances and involve a nonlinear parameter β. With a configuration interaction approach, it is possible to generate highly correlated wave functions for S bound states of heliumlike atoms. Even when a limited number of configurations is included, rather good energy values for the ground and excited states are obtained [36,38]; a systematic improvement is obtained by the inclusion of more configurations. The linear coefficients of the configuration interaction approach are obtained by solving a generalized eigenvalue problem (see [36,38] for more details). By construction, the states obtained form an orthogonal set and satisfy all two-body cusp conditions, and hence deal exactly with the three Coulomb singularities.

Generally, if a trial wave function, which satisfies cusp conditions, is multiplied by a function $\Omega(r_1,r_2,r_{12})$ such that it behaves as $\Omega(r_1,r_2,r_{12})\to 1+O(r_1^2,r_2^2,r_{12}^2)$ near the two-particle coalescence points, the new function also complies with Kato's conditions. This can be easily achieved with a function $\Omega(r_1,r_2,r_{12})$ given as a power series as long as the first power of the coordinates is not included. This technique was successfully employed with the $\phi^{\mathrm{GR}}_{n_1,n_2}$ basis to construct wave functions for two-electron atoms [38–40].

Here we propose to use it also for the diagonal functions $\phi^{\mathrm{C3}}_{n_1,n_2,n_{12}}$ (see also [40]). Hence, we construct the following two trial wave functions:

$$\Psi^{\mathrm{C3}N} = \mathcal{N}\sum_{n_1,n_2,n_{12}} \phi^{\mathrm{C3}}_{n_1,n_2,n_{12}} \sum_{ijk\neq 1} c^{n_1n_2n_{12}}_{ijk} r_1^i r_2^j r_{12}^k, \tag{10}$$

$$\Psi^{\mathrm{GR}N} = \mathcal{N}\sum_{n_1,n_2} \phi^{\mathrm{GR}}_{n_1,n_2} \sum_{ijk\neq 1} c^{n_1n_2}_{ijk} r_1^i r_2^j r_{12}^k, \tag{11}$$

where $\mathcal{N}$ stands for the overall normalization factor (the N in the labels C3N and GRN indicates the number of linear coefficients included).

Since we are interested here only in the ground state, the best compromise—between energy precision and the number of terms—is found when taking only $n_1=1$ and $n_2=1$ (if one should also study excited states, other n_1sn_2s configurations should be included; see [36]), and $n_{12}=1,2$ for the $\Psi^{\mathrm{C3}N}$ functions. We thus consider the following trial wave functions:

$$\Psi^{\mathrm{C3}N} = \mathcal{N}e^{-Z(r_1+r_2)}\left[\left(1+\frac{r_{12}}{2}\right)\sum_{ijk\neq 1} c^{111}_{ijk} r_1^i r_2^j r_{12}^k + \left(1+\frac{r_{12}}{2}+\frac{r_{12}^2}{24}\right)\sum_{ijk\neq 1} c^{112}_{ijk} r_1^i r_2^j r_{12}^k\right], \tag{12}$$

$$\Psi^{\mathrm{GR}N} = \mathcal{N}e^{-Z(r_1+r_2)}\frac{2\beta+1-e^{-\beta r_{12}}}{2\beta}\sum_{ijk\neq 1} c^{11}_{ijk} r_1^i r_2^j r_{12}^k. \tag{13}$$

We have selected some of them, which involve a reasonable number of terms and, at the same time, yield quite accurately the ground state energy. For the GRN wave functions, the linear coefficients c^{11}_{ijk}, the nonlinear parameter β, the normalization factors, and the ground state energies have been given in Table 4 of [38]; here we shall use the three functions with $N=9$ ($E_{\mathrm{GR}9}=-2.903\,27$), $N=14$ ($E_{\mathrm{GR}14}=-2.903\,42$), and $N=29$ ($E_{\mathrm{GR}29}=-2.903\,60$). In Table I, we provide the linear coefficients $c^{11n_{12}}_{ijk}$, the normalization factors, and the ground state energies, for three C3N wave functions for helium ($N=6,12,14$). With both sets of wave functions, the corresponding ground state energies converge progressively towards the numerically exact value [41] as N increases. In Sec. III, we shall also consider the heliumlike ions H^-, and Li^+ up to F^{7+}. As we found that the cross sections calculated with GRN or C3N initial states are not much different when N is sufficiently large, we have chosen to present our results with the best C3N function provided here, i.e., $\Psi_{\mathrm{C3-14}}$. The linear coefficients $c^{11n_{12}}_{ijk}$, the normalization factors $\mathcal{N}$, and the ground state energies for these targets are given in Table II.

C. Numerical technique

To calculate the integral (3), rather than using a direct six-dimensional numerical quadrature, which is computationally expensive, we take advantage of the analytical form of the integrand. Indeed, with either type of initial state wave function (GRN or C3N), the integrand contains only exponentials and powers of the coordinates r_1, r_2, and r_{12} so that one may reduce the six-dimensional numerical quadrature to a two-dimensional one. The method is based on the computation of the term $D=e^{-ar_1}e^{-br_2}e^{-cr_{12}}/(r_1r_2r_{12})$ whose third-order derivative (with respect to a, b, and c) yields the simple function $e^{-ar_1}e^{-br_2}e^{-cr_{12}}$. Thus we rewrite each of the terms $r_1^i r_2^j r_{12}^l e^{-ar_1}e^{-br_2}e^{-cr_{12}}$ appearing in Ψ_i as a mixed derivative of D of order $K=i+j+l+3$. We calculate them using

TABLE I. Linear coefficients $c_{ijk}^{11n_{12}}$, the normalization factors $\mathcal{N}$, and the ground state energies for helium ($Z=2$), corresponding to three C3N wave functions Ψ^{C3N} with $N=6$, 12, and 14.

	$\Psi^{C3\text{-}6}$	$\Psi^{C3\text{-}12}$	$\Psi^{C3\text{-}14}$
$\mathcal{N}$	5.138720	12.50438	14.34774
c_{000}^{111}	0.8213211	0.7370965	0.7019935
c_{200}^{111}	0.0922038	0.0898866	0.1521548
c_{220}^{111}		−0.1400670	−0.1718711
c_{300}^{111}			0.0017437
c_{400}^{111}	0.0025777		
c_{002}^{111}		0.0274772	0.0203784
c_{202}^{111}		0.0001778	0.0006772
c_{222}^{111}		−0.0032172	−0.0043226
c_{000}^{112}	−0.5495211	−0.6266880	−0.6054576
c_{200}^{112}	−0.0567421	−0.0689263	−0.1361976
c_{220}^{112}		0.1324576	0.1647337
c_{300}^{112}			0.0007997
c_{400}^{112}	−0.0011150		
c_{002}^{112}		−0.0189300	−0.0100536
c_{202}^{112}		0.0004286	0.0002263
c_{222}^{112}		0.0014618	0.0020219
$\langle -E \rangle$	2.9019	2.90314	2.90337
$\langle -E \rangle_{exact}$	2.903724		

the automatic differentiation tool Rapsodia [42,43] that provides high-order derivative computations in complex arithmetic. The details and efficiency of the method have been illustrated in [44].

It should be underlined that the use of a two-dimensional quadrature is a great advantage. It allows us to calculate differential cross sections within the second Born approximation (as done, for example, in Ref. [28]), which would be otherwise numerically prohibitive. We recall here that, for the ionization of an atom or a molecule, the second Born approximation is necessary if one wants to take into account the two-step mechanisms, which are particularly important at lower incident energies (see, e.g., [45,46]).

III. RESULTS

A. Helium

We have calculated FDCS for helium within the 3C model and with the initial ground state wave functions given in the previous section. The kinematical situations are those of the only absolute coplanar $(e,3e)$ measurements [2]: incident energy $E_i=5599$ eV, two ejected electrons detected with equal energy (10 eV), and the projectile is scattered with an angle of $\theta_0=0.45°$ (small momentum transfer of $q=0.24$ a.u.); the cross sections were measured at 20 angles θ_1 of one of the ejected electrons as a function of the angle θ_2 of the other ejected electron (all angles are measured in the same sense with respect to the incident beam direction). For illustration purposes, we have selected the two ejected angles θ_1, which correspond to the direction of the momentum transfer $\theta_1=\theta_q=319°$ and its opposite $\theta_1=139°$; similar results are found for 16 out of 20 geometrical situations presented in Ref. [2]. Our calculated FDCSs are plotted in Fig. 1. For both cases, the left (right) panels—presented on the same scale—correspond to the use of Ψ^{GRN} (Ψ^{C3N}) initial wave functions. Small magnitude variations are observed with varying N; all results are, however, similar, within a class and between the two classes of initial states (the results obtained with the best functions, shown with solid lines are even seen to merge at zero degrees in the top panel).

TABLE II. Linear coefficients $c_{ijk}^{11n_{12}}$, the normalization factors $\mathcal{N}$, and the ground state energies for H^- ($Z=1$), and Li^+ ($Z=3$) up to F^{7+} ($Z=9$), corresponding to the wave function $\Psi^{C3\text{-}14}$.

	H^-	Li^+	Be^{2+}	B^{3+}	C^{4+}	N^{5+}	O^{6+}	F^{7+}
$\mathcal{N}/(4Z^3)$	0.0374172	1.48981	4.82531	14.6963	38.9182	90.6382	190.489	369.076
c_{000}^{111}	−0.8973923	0.5222125	0.2903529	0.1483667	0.0800407	0.0463863	−0.0286010	0.0185499
c_{200}^{111}	−0.0415472	0.1788254	0.1417413	0.0972278	0.0675705	0.04893533	−0.0368282	0.0286103
c_{220}^{111}	0.0590762	−0.4325322	−0.6184454	−0.6786570	−0.6950873	−0.6995784	0.7003351	−0.6996425
c_{300}^{111}	0.0508682	0.0081242	0.0087077	0.0071055	0.0055805	0.0044367	−0.0035965	0.0029691
c_{002}^{111}	0.0875540	0.0346836	0.0293156	0.02010317	0.0136315	0.0095273	−0.0068844	0.0051234
c_{202}^{111}	0.0068327	0.0024414	0.0025570	0.0019397	0.00135696	0.0009219	−0.0006078	0.0003799
c_{222}^{111}	0.0004985	−0.0182506	−0.0369923	−0.0528111	−0.0667786	−0.0801030	0.0931841	−0.1061381
c_{000}^{112}	0.3983318	−0.4860190	−0.2779669	−0.1440492	−0.0783453	−0.0456379	0.0282376	−0.0183593
c_{200}^{112}	−0.0079989	−0.1699190	−0.1376899	−0.0954659	−0.0667415	−0.0485088	0.0365916	−0.0284709
c_{220}^{112}	−0.0527623	0.4240615	0.6117701	0.6741871	0.6920865	0.6974908	−0.6988301	0.6985237
c_{300}^{112}	−0.0551156	−0.0066679	−0.0080166	−0.0067890	−0.0054232	−0.0043512	0.0035464	−0.0029381
c_{002}^{112}	−0.0845409	−0.0242275	−0.0225054	−0.0162567	−0.0114064	−0.0081695	0.0060131	−0.0045402
c_{202}^{112}	−0.0019394	−0.0001095	−0.0001227	0.0000195	0.0001599	0.0002667	−0.0003426	0.0003947
c_{222}^{112}	−0.0001276	0.0104637	0.0237988	0.0366252	0.0488337	0.0609381	−0.0730922	0.0853106
$\langle -E \rangle$	0.526438	7.27948	13.6551	22.0304	32.4057	44.7809	59.156	75.5311
$\langle -E \rangle_{exact}$	0.5277	7.2799	13.6556	22.0309	32.4062	44.7814	59.1566	75.5317

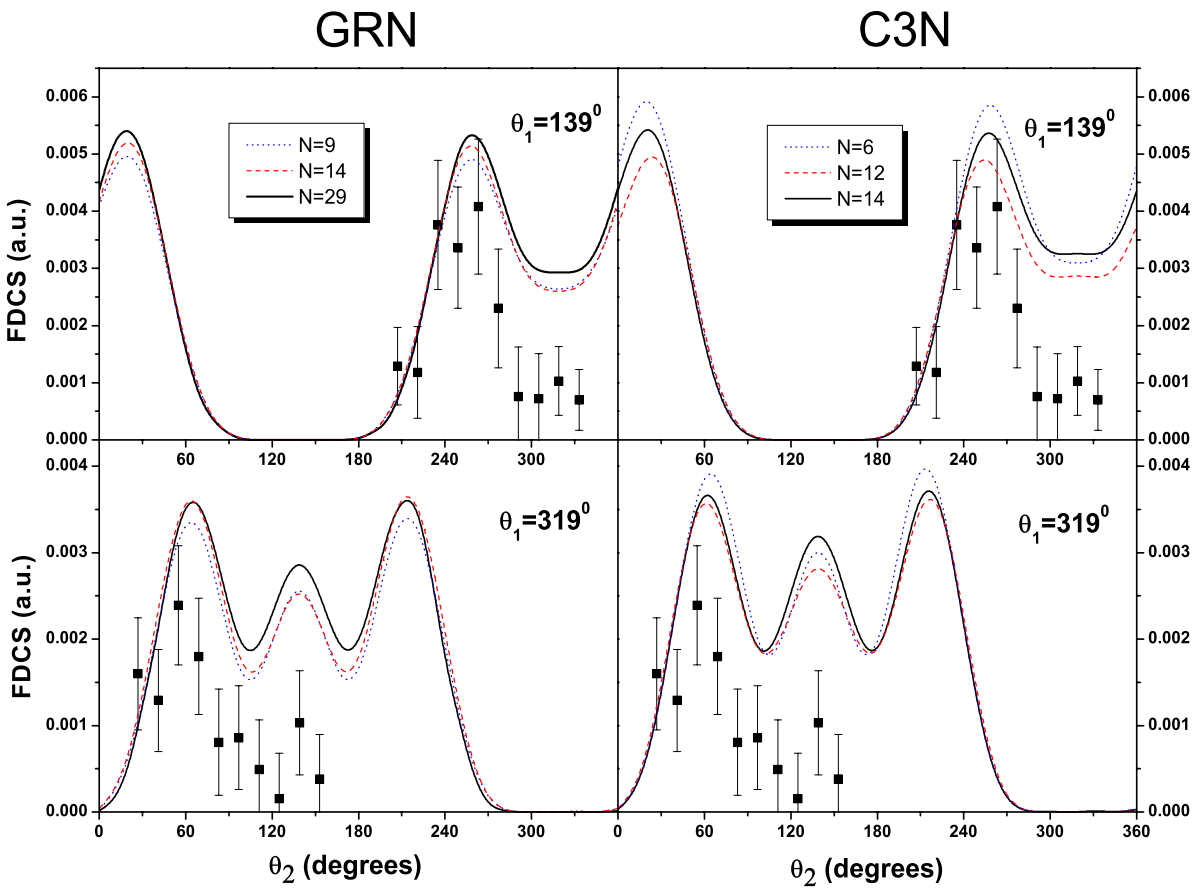

FIG. 1. (Color online) Fivefold differential cross section (FDCS) for $(e,3e)$ ionization of the helium ground state, as a function of the angle of one of the ejected electrons θ_2, with $\theta_1=\theta_q=319°$ (bottom panels) and $\theta_1=\theta_q-180°=139°$ (top panels). The incident electron (at 5599 eV) is scattered at 0.45°, and the two ejected electrons escape with equal energy (10 eV). The absolute experimental data [2] are shown with full squares. The calculated FDCSs are obtained within the C3 model and several initial state wave functions: with $\Psi^{\mathrm{GR}N}$ (left panels) and with $\Psi^{\mathrm{C3}N}$ (right panels) initial wave functions.

As mentioned in the Introduction, the FDCS obtained with highly correlated ground state wave functions reproduce rather well the shapes, but have a magnitude 1.5 to 2 larger than the experimental data. Our results confirm this trend. The improvement of the ground state energy, which intrinsically means a better description of the correlations, does not have much influence on the results. Moreover, if we compare the present results with those (not shown here) obtained with other trial wave functions, which do not satisfy cusp conditions exactly, we see that no substantial differences appear.

Hence, it can be concluded that, when combined with the 3C model, whether the initial state satisfies Kato cusp conditions or not does not matter in these high incident energy $(e,3e)$ processes with the two electrons escaping at 10 eV. This can be related to what is known from studies of double photoionization for which the cusp conditions have fundamental importance at high energy regimes [8] (the electron-nucleus and electron-electron cusp conditions playing a role at different energy regimes). For two electrons ejected with relatively low energy (10 eV) in a $(\gamma,2e)$, and thus similarly for a $(e,3e)$, process we do not expect the electron-electron cusp behavior to play a crucial role.

B. Other heliumlike ions

We now turn to the study of $(e,3e)$ processes on heliumlike ions. When the target is charged, the incident and scattered electrons should be described by Coulomb waves, rather than plane waves, as they feel the long range Coulomb field. This adds an extra difficulty to the theoretical model. If, however, the incident and scattered energies are sufficiently high, the corresponding Sommerfeld parameters are sufficiently small, and the results should not be much affected. We shall thus neglect this effect, and use the final state model described in Sec. II. As double bound initial states we take here the $\Psi^{\mathrm{C3-14}}$ wave functions; we have checked that the results do not vary much when using other $\Psi^{\mathrm{C3}N}$ or $\Psi^{\mathrm{GR}N}$ wave functions, as illustrated above for helium.

As there are no measured data for these targets, the choice of geometrical and kinematical situations is not dictated by the experiments. Within the coplanar geometry and for two electrons ejected with equal energy $E_1=E_2=10$ eV, many possibilities for E_0 (or E_i) and θ_0 can be considered. In what follows we shall select three different choices. The first two are related to previously published results, while the third one is a new proposal. To make the reading easier, the geo-

TABLE III. Kinematical and geometrical conditions corresponding to Figs. 2–5.

	Target	E_0 (eV)	$E_1=E_2$ (eV)	θ_0 (deg)	q (a.u.)	θ_q (deg)
Fig. 2	H^-	5500	10	0.45	0.24	292
	He	5500	10	0.45	0.17	319
	Li^+	5500	10	0.45	0.43	338
Fig. 3	H^-	5565	10	0.656	0.24	285
	He	5500	10	0.45	0.24	319
	H^-	5565	10	1.203	0.43	279
	He	5500	10	1.108	0.43	295
	Li^+	5381	10	0.457	0.43	338
	H^-	5565	10	5.600	1.98	275
	He	5500	10	5.596	1.98	278
	Li^+	5381	10	5.534	1.98	284
Fig. 4	H^-	660	10	1.298	0.24	319
	He	5500	10	0.45	0.24	319
	Li^+	26741	10	0.204	0.24	319
	H^-	704	10	3.097	0.43	295
	He	5500	10	1.108	0.43	295
	Li^+	26218	10	0.507	0.43	295
Fig. 5	H^-	937.6	1.706	0.45	0.10	319
	He	5500	10	0.45	0.24	319
	Li^+	13851.7	25.183	0.45	0.38	319
	Be^{2+}	25992.6	47.256	0.45	0.52	319
	B^{3+}	41922.9	76.219	0.45	0.66	319
	C^{4+}	61642.4	112.07	0.45	0.80	319
	N^{5+}	85151.8	154.81	0.45	0.94	319
	O^{6+}	112450.5	204.44	0.45	1.08	319
	F^{7+}	143538.8	260.96	0.45	1.22	319

metrical and kinematical values of all cases investigated here are summarized in Table III.

A first choice is to keep for other heliumlike ions the same conditions as those used in the measurements for helium [2], i.e., $E_0=5500$ eV and $\theta_0=0.45°$. This is actually what was proposed in the paper by Lamy *et al.* [30], where H^- and He were studied under the same conditions (which are similar to those of the experiments [2] performed a few years later). Since the double ionization energies change with the target's nuclear charge Z, the modulus and the direction of the momentum transfer $\mathbf{q}$ change (see Table III, entry Fig. 2). For illustration purposes, we take one of the ejected electrons taken in the direction of the momentum transfer ($\theta_1=\theta_q$), and in Fig. 2 we plot the calculated FDCSs for H^-, He, and Li^+ versus the $\theta_2-\theta_q$. This artificial rotation, which is different for each target, facilitates the visual comparison as the symmetry with respect to θ_q is restored. In order to put all results on the same scale, the FDCS for H^- has been divided by 200, and that of Li^+ multiplied by 100; the helium data are those reported in Fig. 1. Similarly to them, the FDCS for H^- and Li^+ present two maxima approximately in the direction perpendicular to the momentum transfer. The fact that the cross section for H^- is much larger than for helium has been observed already in Ref. [30]; actually, our results are very

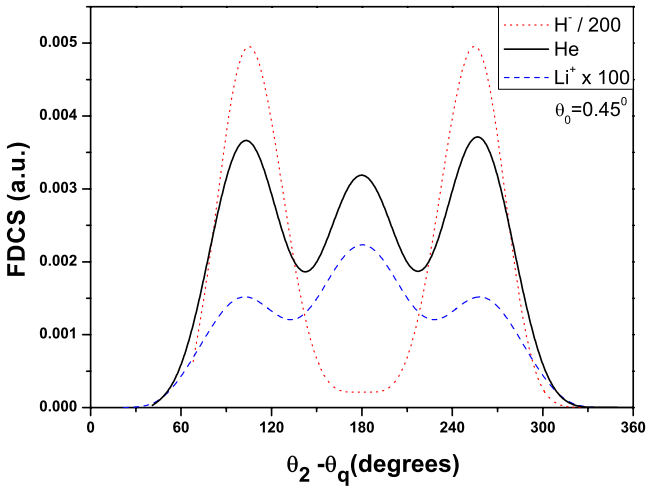

FIG. 2. (Color online) Fivefold differential cross section (FDCS) for $(e,3e)$ ionization of the H^-, He, and Li^+ ground states, calculated with the 3C model and the Ψ^{C3-14} initial state wave function, as a function of the angle of one of the ejected electrons $\theta_2-\theta_q$. The other electron is detected at $\theta_1=\theta_q$ (see Table III). The scattered electron takes 5500 eV and the direction $\theta_0=0.45°$; the two ejected electrons escape with equal energy $E_1=E_2=10$ eV. The FDCS for H^- (dotted line) is divided by 200 and that for Li^+ (dashed line) is multiplied by 100, while for He (solid line) it is shown on absolute scale.

similar to theirs, the difference being related to their use of a different (poorer) initial state, and slightly different geometrical and kinematical conditions. The figure also shows that the Li^+ cross sections are much smaller than for helium; this has been observed in [34] but with a simplified 3C model, the 2CG model. It should be noticed here that our FDCSs differ substantially from those of [34], not only in the magnitude but also in the angular distribution. We should also add that the Gamow factor related to α_{12} plays an important role for two electrons ejected at 10 eV, as its square modulus peaks at $\theta_2=\theta_q-180°$ and is responsible for the central peak.

A second choice, considered by Muktavat and Srivastava [34], is to keep the same incident energy ($E_i=5599$ eV) for all targets, but change the scattering angle θ_0 in such a way that the modulus q is kept constant; the direction of $\mathbf{q}$, however, changes (see Table III, entry Fig. 3). In order to observe any dependence on the momentum transfer q, we consider three of the values chosen in [34]: $q=0.24$, $q=0.43$, and $q=1.98$ a.u. (note that it is not possible to find a θ_0 value corresponding to $q=0.24$ a.u. in the case of Li^+). In Fig. 3 we plot the FDCS calculated for $\theta_1=\theta_q$, as a function of $\theta_2-\theta_q$; each panel corresponds to a value of q, and cross sections are multiplied for Li^+ or divided for H^- by factors as indicated. As the value of q increases, the FDCS magnitude decreases and the angular distributions change. For the largest value considered a unique maximum appears; this maximum is related to the domination of the electron-electron Gamow factor, which peaks at 180°. Once again our 3C results differ substantially, in both magnitude and shapes, from those of [34] obtained with the 2CG model.

A third choice, proposed here, is to choose the scattered energy E_0 and the scattering angle θ_0 in such a way that the

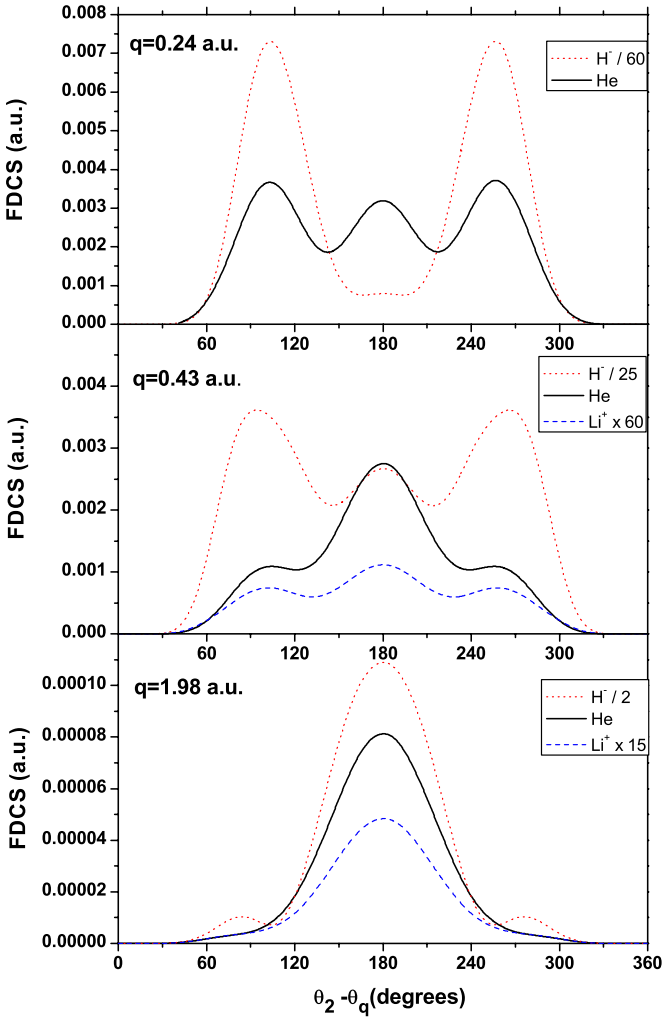

FIG. 3. (Color online) Fivefold differential cross section (FDCS) for $(e,3e)$ ionization of the H^-, He, and Li^+ ground states, calculated with the 3C model and the Ψ^{C3-14} initial state wave function, as a function of the angle of one of the ejected electrons $\theta_2-\theta_q$. The other electron is detected at $\theta_1=\theta_q$. Both ejected electrons escape with equal energy $E_1=E_2=10$ eV. The scattered electron takes energy E_0 and goes in the direction θ_0 in order to keep the modulus q constant (see Table III). FDCSs for H^- (dotted lines) and Li^+ (dashed lines) are divided or multiplied as indicated in each of the three panels, which correspond to $q=0.24$ a.u., $q=0.43$ a.u., and $q=1.98$ a.u.; the FDCSs for He (solid lines) are shown on absolute scale.

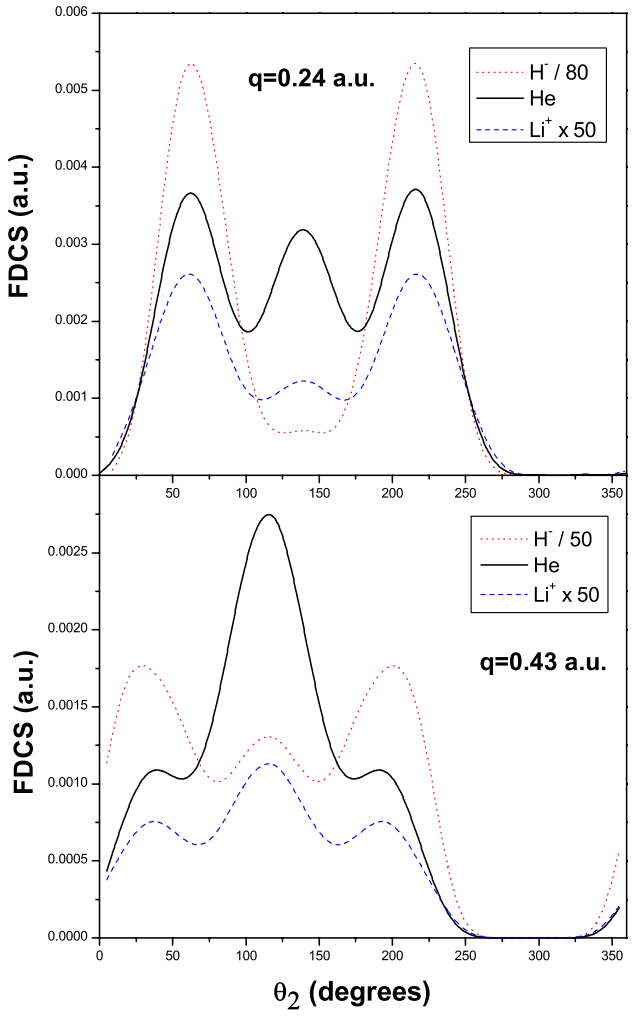

FIG. 4. (Color online) Fivefold differential cross section (FDCS) for $(e,3e)$ ionization of the H^-, He, and Li^+ ground states, calculated with the 3C model and the Ψ^{C3-14} initial state wave function, as a function of the angle of one of the ejected electrons θ_2. The other electron is detected at $\theta_1=\theta_q$. Both ejected electrons escape with equal energy $E_1=E_2=10$ eV. The scattered electron takes energy E_0 and goes in the direction θ_0 in order to keep the vector **q** constant (see Table III). The cross sections for H^- and Li^+ are divided or multiplied as indicated; the two panels correspond to $q=0.24$ a.u. and $q=0.43$ a.u.

momentum transfer **q** is kept constant, in both modulus and direction. Two values of q are considered (see Table III, entry Fig. 4): $q=0.24$ a.u. (the value of the helium experiments [2]) and $q=0.43$ a.u. At the same time the ejected energies are not varied (10 eV for each electron) so that the large effect of the Gamow factor linked to α_{12} is kept unvaried for all targets. In this way, the cross sections for different targets will depend only on the target wave functions and on the Sommerfeld parameters α_j connected to the two ejected electrons. In Fig. 4, our calculated FDCSs are plotted, versus θ_2, again for H^-, He, and Li^+, and for $\theta_1=\theta_q=319°$, $q=0.24$ a.u. (top panel) and $\theta_1=\theta_q=295°$, $q=0.43$ a.u. (bottom panel). They all present the same symmetry with respect to the direction of the momentum transfer (no artificial rotation is thus necessary). With the chosen kinematical and geometrical situation, the cross section's magnitude will be mainly governed by the initial wave function Ψ_i, i.e., by the nuclear charge Z. In order to put all cross sections on the same scale as for helium we had to multiply those of Li^+ and divide those for H^- as indicated in each panel.

C. Approximate scaling law

Cross sections for positive ions decrease with increasing values of the nuclear charge Z and it is interesting to search for a scaling law. To do this one should take appropriately scaled kinematical conditions. The presence of several ingredients in formula (1) for the FDCS, however, indicates that

no exact scaling can be found. First of all, the initial states do not scale with Z. Secondly, it is impossible to find kinematic conditions in order to keep the 3C model for the final state double continuum unchanged for several heliumlike ions; indeed, while it is possible to choose $E_1=E_2$ to keep the Sommerfeld parameters α_j $(j=1,2)$ constant, one cannot fix—at the same time—α_{12}, i.e., the parameter related to the electron-electron interaction. For these two reasons, only an approximate scaling law can be proposed, and we shall use a methodology similar to that presented in [47] for $(e,2e)$ processes.

We start with two preliminary considerations concerning the two-electron initial states. First of all, their double ionization potentials $\mathcal{P}_{(\mathrm{DI})}$ can be well represented by a one-parameter fit

$$\mathcal{P}_{\mathrm{DI}} = -A\tilde{z}^2, \tag{14}$$

where $A=0.996$ and $\tilde{z}=Z-0.2962$, the worst fit being for $Z=1$ (note that, to be consistent, we have used the $\mathcal{P}_{\mathrm{DI}}$ corresponding to the $\Psi^{\mathrm{C3-14}}$ wave functions and not the exact values; anyhow, only tiny differences are observed). The validity of the fit is better justified as Z increases. Note also that the value 0.2962 is not far from the well-known Slater screening value of 0.3. Secondly, to a very rough approximation, the $\Psi^{\mathrm{C3-14}}$ wave functions for any target (Z) are given by the product of two hydrogenic exponentials multiplied by a prefactor $\mathcal{N}(Z)$. The latter can be well fitted by the following power law in $\tilde{z}$:

$$\mathcal{N}(Z) = B\tilde{z}^{\beta}, \tag{15}$$

with $B=0.070\,06$ and $\beta=3.054\,45$. Note that the β value is not far from 3, which would be the power of the independent particle model.

Consider now two ions, of nuclear charges $Z^{(N)}$ and $Z^{(M)}$, belonging to the helium isoelectronic sequence, and define the ratio

$$\gamma^{NM} = \frac{\tilde{z}^{(N)}}{\tilde{z}^{(M)}}. \tag{16}$$

Although the two-electron wave functions Ψ_i do not scale exactly, in view of Eq. (15) and of the hydrogenic exponentials presence, we shall make the assumption that the relation

$$\Psi_i^{(N)}([\gamma^{NM}]^{-1}r_1,[\gamma^{NM}]^{-1}r_2,[\gamma^{NM}]^{-1}r_{12}) \simeq (\gamma^{NM})^{\beta}\Psi_i^{(M)}(r_1,r_2,r_{12}) \tag{17}$$

holds true. As $Z^{(N)}$ increases with respect to $Z^{(M)}$, this scaling relation holds relatively better. However, this approximation will be one of the sources of scaling law breaking.

Consider an $(e,3e)$ process on a heliumlike ion, labeled M, in which the incident electron energy is X times the $\mathcal{P}_{\mathrm{DI}}$ of the target ion, i.e., $E_i^{(M)}=X|\mathcal{P}_{\mathrm{DI}}^{(M)}|$, and the two ejected electrons escape with energies $E_1^{(M)}$ and $E_2^{(M)}$. The energy conservation is expressed by

$$E_i^{(M)} = E_0^{(M)} + E_1^{(M)} + E_2^{(M)} - \mathcal{P}_{\mathrm{DI}}^{(M)}, \tag{18}$$

where, according to the proposed fit, $\mathcal{P}_{\mathrm{DI}}^{(M)}$ is given by Eq. (14). Consider now an $(e,3e)$ process on another ion, labeled by N, with the same incident energy to $|\mathcal{P}_{\mathrm{DI}}|$ ratio X. We may write the following energy and momentum scaling relations:

$$E_i^{(N)} = X|\mathcal{P}_{\mathrm{DI}}^{(N)}| = (\gamma^{NM})^2 E_i^{(M)}, \tag{19}$$

$$k_i^{(N)} = \gamma^{NM} k_i^{(M)}, \tag{20}$$

where γ^{NM} is given by Eq. (16). If we take the energy of the ejected electrons from ion N to be

$$E_j^{(N)} = (\gamma^{NM})^2 E_j^{(M)} \quad (j=1,2), \tag{21}$$

which also means $k_j^{(N)}=\gamma^{NM}k_j^{(M)}$, then we also have $k_0^{(N)}=\gamma^{NM}k_0^{(M)}$ because of the energy conservation (18).

Let us now look at the Sommerfeld parameters, which characterize the 3C model for the final state. For each ion, the electron-nucleus interaction corresponds to $-Z$ while the electron-electron repulsion corresponds to 1. With these charges, the three Sommerfeld parameters α_1, α_2, and α_{12} cannot be kept equal for two ions M and N. Of course $\alpha_{12}^{(N)} \neq \alpha_{12}^{(M)}$; on the other hand, as Z increases, it follows from the scaling relation (21) that

$$\alpha_j^{(N)} \simeq \alpha_j^{(M)} \quad (j=1,2). \tag{22}$$

These facts will be another source of breaking the scaling law.

With these considerations in mind, let us now turn to formula (1) for the differential cross sections. Under the chosen scaled kinematical conditions, and assuming relation (22) holds true, the final state does not change except for the electron-electron interaction distortion factor. The FDCS for two ions N and M can then be mathematically related through a change of variables of the radial coordinates, i.e., r into $[\gamma^{NM}]^{-1}r$ for the three Hylleraas coordinates r_1, r_2, and r_{12}. It is then straightforward to establish the following approximate scaling law:

$$\frac{d^5\sigma^{(N)}}{d\Omega_0 d\Omega_1 d\Omega_2 dE_1 dE_2}[(\gamma^{NM})^2E_i^{(M)},(\gamma^{NM})^2E_1^{(M)},(\gamma^{NM})^2E_2^{(M)}] \simeq (\gamma^{NM})^{6\beta-26}\frac{d^5\sigma^{(M)}}{d\Omega_0 d\Omega_1 d\Omega_2 dE_1 dE_2}[E_i^{(M)},E_1^{(M)},E_2^{(M)}], \tag{23}$$

where $6\beta-26\simeq-7.673$. This relation is derived by considering for the final state (7), only the dominant second term, which arises from the orthogonalization procedure. The first term would give FDCSs scaled as $(\gamma^{NM})^{2\beta-14}$; since $2\beta-14 \simeq -7.891$ the first term scales in approximately the same fashion. Within the independent particle model, on the other hand, $\beta=3$ and $6\beta-26=2\beta-14=8$, so that cross sections would scale as $(\gamma^{NM})^{-8}$.

To check the validity of the proposed approximate scaling law, we have calculated 3C FDCSs for several two-electron ions keeping the scattered angle fixed at $\theta_s=0.45$. The kinematical conditions, scaled with respect to the helium $(M=2)$ experimental conditions, are given in Table III. Notice that as Z increases the incident energy becomes quite large; for even larger values of Z relativistic effects should be considered but this goes far beyond the scope of the present study. Since k_i and k_0 are equally scaled, the momentum

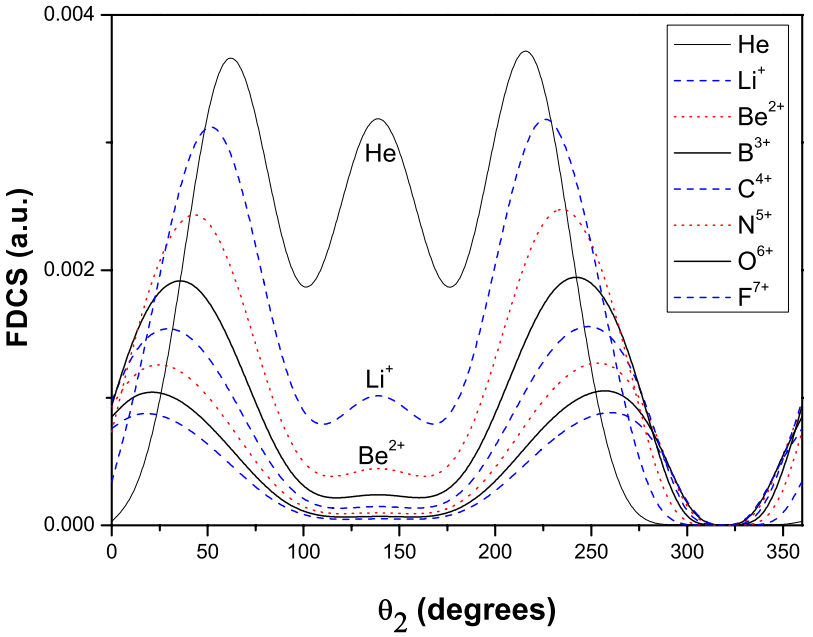

FIG. 5. (Color online) Fivefold differential cross section (FDCS) for $(e,3e)$ ionization of the helium atom, and the heliumlike positive ions Li^+ up to F^{7+} ground states, as a function of the angle of one of the ejected electrons θ_2. The scattered electron goes in the direction $\theta_0=0.45$, while the other ejected electron is detected at $\theta_1=\theta_q$. Both ejected electrons escape with equal energy $E_1=E_2$ as indicated in Table III. The FDCSs are calculated with the 3C model and the Ψ^{C3-14} initial state wave function. The cross section for helium is shown on an absolute scale, while for the heliumlike positive ions the FDCSs are multiplied by the factor $(\gamma^{N2})^{-6\beta+26}$ according to the approximate scaling law (23).

transfer q scales as γ^{N2} but its direction is the same for all ions; the shapes of the cross sections should therefore all have the same symmetry. The corresponding FDCSs are shown in Fig. 5: for helium $(Z=2)$, the FDCSs is shown on an absolute scale, while for the positive ions with $Z>2$ the magnitudes, which decrease very rapidly with increasing nuclear charges, are rescaled according to Eq. (23), i.e., multiplied by the factor $(\gamma^{N2})^{-6\beta+26}$.

From Fig. 5 we observe that the FDCS shapes are approximately similar for all two-electron atoms. As Z increases, the momenta k_1 and k_2 increase so that the distortion factor of the 3C model related to α_{12}, which is not scaled, plays a relatively minor role; the related central peak is indeed relatively smaller. We also observe that, once rescaled, all FDCSs can be viewed on the same graph. It should be underlined that, for example, the C^{4+} cross sections are about a factor 10^4 smaller than for neutral helium. Of course, some magnitude and shape differences exist between the scaled FDCSs. One should not forget that the scaling law is based on several assumptions. As Z increases these assumptions are better verified, and indeed the curves with higher Z get closely bunched together.

If instead of the pure 3C model we consider effective charges $-\tilde{z}=-(Z-0.2962)$ for both electron-nucleus interactions (note that they do not correspond to the correct asymptotic behavior), relation (22) is exactly verified, and consequently the FDCS scaling (23) is better verified. We have carried out the corresponding calculations: only a small improvement was observed.

One last observation; for very large Z our ratio γ^{N2} tends to the ratio of nuclear charges $Z^{(N)}/2$; within the independent particle model, $\beta=3$, the scaling law (23) becomes $(Z^{(N)}/2)^{-8}$. This result is similar to those presented for $(e,2e)$ [9] and $(\gamma,2e)$ [10,11] processes on heliumlike ions. In these publications, the scaling of the triple differential cross sections goes as $(Z^{(N)}/2)^{-6}$. On the other hand, for H-like and alkalilike ions, it was shown [47] that the $(e,2e)$ triple differential cross sections are related by a factor $(\gamma^{NM})^{2\beta-9}$, where β and the effective charges $\tilde{z}$ take specific values for each sequence.

IV. SUMMARY

We have calculated $(e,3e)$ cross sections for several heliumlike ions, within the 3C model and with several highly correlated bound wave functions, which fulfill exactly Kato cusp conditions. It emerges that the behavior of the ground state wave function near the two-body coalescence points has little influence in the experimental high energy conditions, thus definitively confirming the conclusions of Chuluunbaatar *et al.* [15].

Under similar kinematical and geometrical conditions, the H^- cross sections are predicted to be much larger than for helium, while for heliumlike positive ions they decrease fast with increasing nuclear charges. We have presented, for the first time, proper 3C results for heliumlike positive ions.

Using the analyticity of the 3C final state, an approximate scaling law for $(e,3e)$ FDCS is mathematically identified by choosing properly scaled energies. Our calculations show that the scaling is well verified. It can be used to easily predict cross sections, which are extremely difficult to measure.

For the double ionization of negative or positive two-electron ions the collision model should be improved by considering Coulomb waves rather than plane waves for the incident and scattered waves; this would be of significance if lower incident energies should be considered. This extension is a matter for further investigations.

[1] J. Berakdar, A. Lahmam-Bennani, and C. Dal Cappello, Phys. Rep. **374**, 91 (2003).
[2] A. Lahmam-Bennani, I. Taouil, A. Duguet, M. Lecas, L. Avaldi, and J. Berakdar, Phys. Rev. A **59**, 3548 (1999).
[3] A. S. Kheifets *et al.*, J. Phys. B **32**, 5047 (1999).
[4] L. U. Ancarani, G. Gasaneo, F. D. Colavecchia, and C. Dal Cappello, Phys. Rev. A **77**, 062712 (2008).
[5] C. R. Garibotti and J. E. Miraglia, Phys. Rev. A **21**, 572 (1980); M. Brauner, J. Briggs, and H. Klar, J. Phys. B **22**, 2265 (1989).
[6] B. Joulakian, C. Dal Cappello, and M. Brauner, J. Phys. B **25**, 2863 (1992).
[7] T. Kato, Pure Appl. Math. **10**, 151 (1957).
[8] T. Suric, E. G. Drukarev, and R. H. Pratt, Phys. Rev. A **67**, 022709 (2003).
[9] A. L. Frapiccini, K. V. Rodriguez, G. Gasaneo, and S. Otranto, Braz. J. Phys. **37**, 1115 (2007).
[10] M. A. Kornberg and J. E. Miraglia, Phys. Rev. A **49**, 5120 (1994).
[11] S. Otranto and C. R. Garibotti, Eur. Phys. J. D **27**, 215 (2003).
[12] R. A. Bonham and D. A. Kohl, J. Chem. Phys. **45**, 2471 (1966).
[13] T. Kinoshita, Phys. Rev. **105**, 1490 (1957).
[14] C. Le Sech, J. Phys. B **30**, L47 (1997).
[15] O. Chuluunbaatar, I. V. Puzynin, P. S. Vinitsky, Y. V. Popov, K. A. Kouzakov, and C. Dal Cappello, Phys. Rev. A **74**, 014703 (2006).
[16] A. S. Kheifets and I. Bray, Phys. Rev. A **69**, 050701(R) (2004).
[17] S. A. Zaytsev, V. A. Knyr, and Yu. V. Popov, Phys. At. Nucl. **70**, 676 (2007).
[18] V. A. Knyr, V. V. Nasyrov, and Yu. V. Popov, in *Correlation and Polarization in Photonic, Electronic, and Atomic Collisions*, edited by G. F. Hanne *et al.*, AIP Conf. Proc. No. 697 (AIP, Melville, NY, 2003), p. 76.
[19] V. V. Serov, V. L. Derbov, B. B. Joulakian, and S. I. Vinitsky, Phys. Rev. A **75**, 012715 (2007).
[20] S. Jones and D. H. Madison, Phys. Rev. Lett. **91**, 073201 (2003).
[21] L. U. Ancarani, T. Montagnese, and C. Dal Cappello, Phys. Rev. A **70**, 012711 (2004).
[22] S. Jones, J. H. Macek, and D. H. Madison, Phys. Rev. A **70**, 012712 (2004).
[23] F. D. Colavecchia, G. Gasaneo, and K. V. Rodriguez, J. Electron Spectrosc. Relat. Phenom. **161**, 73 (2007).
[24] L. U. Ancarani and C. Dal Cappello, J. Electron Spectrosc. Relat. Phenom. **161**, 22 (2007).
[25] G. Gasaneo, S. Otranto, and K. V. Rodriguez, *Proceedings of the XXIV International Conference on Photonic, Electronic and Atomic Collision* (World Scientific, Singapore, 2006), p. 360.
[26] L. U. Ancarani, C. Dal Cappello, and T. Montagnese, in *Ionization, Correlation, and Polarization in Atomic Collisions*, edited by A. Lahmam-Bennani and B. Lohmann, AIP Conf. Proc. No. 811 (AIP, Melville, NY, 2006), p. 1.
[27] A. S. Kheifets, Phys. Rev. A **69**, 032712 (2004).
[28] L. U. Ancarani, T. Montagnese, and C. Dal Cappello, in *Electron and Photon Impact Ionization and Related Topics*, edited by B. Piraux, IOP Conf. Proc. No. 183 (Institute of Physics, London, 2005), p. 21.
[29] P. Pluvinage, Ann. Phys. (Paris) **5**, 145 (1950); J. Phys. Radium **12**, 789 (1951).
[30] P. Lamy, C. Dal Cappello, B. Joulakian, and C. Le Sech, J. Phys. B **27**, 3559 (1994).
[31] P. Defrance *et al.*, J. Phys. B **32**, 2227 (1999).
[32] B. Nath and C. Sinha, J. Phys. B **33**, 5525 (2000).
[33] D. Ghosh, B. Nath, and C. Sinha, J. Phys. B **36**, 1479 (2003).
[34] K. Muktavat and M. K. Srivastava, J. Phys. B **34**, 2975 (2001).
[35] B. Nath, R. Biswas, and C. Sinha, Phys. Rev. A **59**, 455 (1999).
[36] G. Gasaneo and L. U. Ancarani, Phys. Rev. A **77**, 012705 (2008).
[37] L. U. Ancarani and G. Gasaneo, Phys. Rev. A **75**, 032706 (2007).
[38] K. V. Rodriguez, G. Gasaneo, and D. M. Mitnik, J. Phys. B **40**, 3923 (2007).
[39] K. V. Rodriguez and G. Gasaneo, J. Phys. B **38**, L259 (2005).
[40] K. V. Rodriguez, V. Y. Gonzalez, L. U. Ancarani, D. M. Mitnik, and G. Gasaneo (to be published).
[41] G. W. F. Drake, *Springer Handbook of Atomic, Molecular, and Optical Physics* (Springer, New York, 2005).
[42] I. Charpentier and J. Utke, Optim. Methods Software (in press).
[43] I. Charpentier, C. Dal Cappello, and J. Utke, *Advance in Automatic Differentiation*, Lecture Notes in Computational Science and Engineering, Vol. 64, edited by C. H. Bischof, H. M. Bücker, P. Hovland, U. Naumann, and J. Utke (Springer, Berlin, 2008), p. 127.
[44] I. Charpentier and C. Dal Cappello, INRIA Report No. RR-5546, 2005 (http://www.inria.fr/rrrt/rr-5546.html).
[45] C. Dal Cappello, R. El Mkhanter, and P. A. Hervieux, Phys. Rev. A **57**, R693 (1998).
[46] J. H. McGuire, Phys. Rev. Lett. **49**, 1153 (1982).
[47] L. U. Ancarani and P. A. Hervieux, J. Phys. B **36**, 4447 (2003).